OXFORD

SOT | Society of Toxicology
www.toxsci.oxfordjournals.org

TOXICOLOGICAL SCIENCES, 149(1), 2016, 227–236

doi: 10.1093/toxsci/kfv230
Advance Access Publication Date: October 26, 2015
Research Article

Skin Damage Mechanisms Related to Airborne Particulate Matter Exposure

Natalia D. Magnani,* Ximena M. Muresan,† Giuseppe Belmonte,† Franco Cervellati,† Claudia Sticozzi,† Alessandra Pecorelli,† Clelia Miracco,‡ Timoteo Marchini,* Pablo Evelson,* and Giuseppe Valacchi,†,§,1

*Institute of Biochemistry and Molecular Medicine (IBIMOL-UBA-CONICET), Pharmacy and Biochemistry School, University of Buenos Aires, Buenos Aires, Argentina; †Department of Life Sciences and Biotechnology, University of Ferrara, Ferrara, Italy; ‡Department of Neuroscience, Medical and Surgical Sciences. University of Siena, Siena, Italy; and §Department of Food and Nutrition, Kyung Hee University, Seoul, South Korea

[1]To whom correspondence should be addressed at Department of Life Sciences and Biotechnology, University of Ferrara, Via Borsari, 46, Ferrara, Italy. Fax: +39 0532 455450. E-mail: vlcgpp@unife.it.

ABSTRACT

Epidemiological studies suggest a correlation between increased airborne particulate matter (PM) and adverse health effects. The mechanisms of PM-health effects are believed to involve oxidative stress and inflammation. To evaluate the ability of PM promoting skin tissue damage, one of the main organs exposed to outdoor pollutants, we analyzed the effect of concentrated ambient particles (CAPs) in a reconstructed human epidermis (RHE) model. RHE tissues were exposed to 25 or 100 μg/ml CAPs for 24 or 48 h. Data showed that RHE seems to be more susceptible to CAPs-induced toxicity after 48 h exposure than after 24 h. We found a local reactive O_2 species (ROS) production increase generated from metals present on the particle, which contributes to lipids oxidation. Furthermore, as a consequence of altered redox status, NFkB nucleus translocation was increase upon CAPs exposure, as well as cyclooxygenase 2 and cytochrome P450 levels, which may be involved in the inflammatory response initiated by PM. CAPs also triggered an apoptotic process in skin. Surprisingly, by transition electron microscopy analysis we showed that CAPs were able to penetrate skin tissues. These findings contribute to the understanding of the cutaneous pathophysiological mechanisms initiated by CAPs exposure, where oxidative stress and inflammation may play predominant roles.

Key words: air pollution; cutaneous tissues; particulate matter; oxidative damage; inflammation

Numerous studies have shown a direct correlation between decreased air quality levels and adverse health effects (Brunekreef and Holgate, 2002; Valacchi *et al.*, 2012). Air pollution is a heterogeneous mixture of chemicals and solid particles, in which chemical composition, size, and sources of origin differ in each microenvironment (Nel, 2005). In the airborne particulate matter (PM) both organic and inorganic compounds could be found in the particle's core as well as in the surface. They are emitted into the atmosphere from natural and anthropogenic sources. Among the wide variety of pollutants, PM, specially particles on the nanosize range, seems to be of major concern from a health perspective, and has been pointed out as an environmental threat not only to susceptible but also to healthy members of the population (WHO, 2014).

Concentrated air particles (CAPs) represent the fraction of atmospheric pollutants with a size range between 0.1 and 2.5 μm, collected by a particles concentrator. Therefore, CAPs have the advantage of allowing "real world PM" exposures (Ghio and Huang, 2004).

The respiratory and oral tracts along with the skin are the common routes by which organisms enter in contact with different ambient pollutants. Because of its critical location, the

skin provides a major interface between the body and the environment, and offers a biological barrier against air PM (Valacchi *et al.*, 2012). However, the skin defensive capacity is not unlimited. Environmental stressors may exceed the protective potential and disturb the skin structure leading to skin diseases, such as erythema, edema, hyperplasia, skin aging, contact dermatitis, atopic dermatitis, psoriasis, and carcinogenesis (Baroni *et al.*, 2012).

Recent epidemiological studies suggest that PM negatively affect human skin (Vierkötter *et al.*, 2010) and exacerbates preexistent skin diseases (Kim *et al.*, 2013). However, information regarding the toxicological mechanisms by which PM can impact on skin function is limited.

In vitro and *in vivo* studies have shown a variety of biological effects after CAPs exposures not only in chronic but also after acute exposures (Gurgueira *et al.*, 2002). The mechanisms by which the PM exerts its detrimental effects are believed to involve oxidative stress and inflammation (Donaldson *et al.*, 2005) both important contributors to extrinsic skin aging (Schröder *et al.*, 2006).

Injury mechanisms after PM exposure have been suggested to involve local reactive O_2 species (ROS) production which could, in part, be generated from the particles themselves. Moreover, smaller particles provide a higher surface area, in which different compounds could be adsorbed (Nel *el al.*, 2006). On the one hand, the oxidative capacity of PM has been attributed to its transition metal constituents, which typically include Fe, V, Cr, Mn, Co, Ni, Cu, Zn, and Ti. Most of these metals can catalyze Fenton-like reactions and generate ROS initiating oxidative damage mechanisms (Chen and Lipmann, 2009). On the other hand, particles can serve as organic compounds carriers like polycyclic aromatic hydrocarbons (PAHs), which are highly lipophilic, and capable of localizing in mitochondria contributing to the reported ROS production (Li *et al.*, 2008). Furthermore, O_2-derived free radicals may also be generated by the interaction of particle pollutants and their components, with cellular enzymes and organelles (Magnani *et al.*, 2013).

Regarding inflammatory responses, it has been observed that systemic proinflammatory cytokines, such as TNF-α and interleukin (IL)-6 became increased after exposures to PM (Marchini *et al.*, 2014). In skin tissues, an increased reactive O_2 production could stimulate a variety of cutaneous cells to release pro-inflammatory mediators, leading to infiltration of activated neutrophils and phagocytic cells which are able to produce even more free radicals (Pillai *et al.*, 2005).

Taking into account that oxidative stress and inflammation play a predominant role in air pollution toxicity, the aim of the present work was to evaluate the ability of CAPs to promote skin tissues oxidative damage and to asses the possible mechanisms involved in this process.

MATERIALS AND METHODS

Experimental Model

CAPs suspension. In this study PM named CAPs were used as particles sample. CAPs are recognized ambient PM and were generously provided by B. Gonzalez-Flecha. They were collected using a virtual concentrator, the Harvard Ambient Particle Concentrator (HAPC), which concentrates ambient air particles for subsequent exposure in different animal models (Harvard School of Public Health, Boston, Massachusetts). The principle of virtual impaction was used to concentrate ambient particles in the size range of 0.1–2.5 μm (fine particles) (Rhoden *et al.*, 2004; Sioutas *et al.*, 1995). CAPs samples from this source have been previously characterized in terms of elemental composition (Ghelfi *et al.*, 2010; Gurgueira *et al.*, 2002). PM suspension was freshly prepared by resuspending CAPs particles in sterile saline solution for reconstructed human epidermis (RHE) exposure or in culture media for cell culture exposure, at final concentrations of 25 or 100 μg/ml, followed by 10 min incubation in an ultrasonic water bath (Goldsmith *et al.*, 1998).

Skin tissues and cells culture exposure. RHE tissues were used as a skin tissue model. EpiDermTM Tissue Model has been purchased to MatTek (MatTek *In Vitro* Life Science Laboratories, Bratislava, Slovak Republic). They were kept at 37°C in a humidified 5% CO_2 atmosphere in a maintenance medium provided by manufacturers until the exposure. Prior to PM exposure, media was aspirated and fresh media was added. For the exposure, 10 μl of PM suspension (25 or 100 μg/ml) was topically applied over the RHE in a single dose (0.5 or 2.0 μg/cm^2, respectively). The selection of the PM doses was based on results shown in previous *in vitro* studies (Fujishima *et al.*, 2013; Mastrofrancesco *et al.*, 2014; Pierdominici *et al.*, 2014; Soeur *et al.*, 2015). Control tissue was exposed to 10 μl of the vehicle (saline). To avoid excess tissue moistening, a minimum suspension volume to deliver the particles was used. After exposure, tissues were also kept at 37°C in a humidified 5% CO_2 atmosphere in a maintenance medium. Measurements were made after 24 or 48 h exposure. Because no differences between 24 and 48 h saline exposure were observed (controls), the samples were pooled and presented as Control group.

In addition, the spontaneously immortalized human keratinocyte HaCaT cell line was used for the cellular experiments. HaCaT cells were culture as previously described (Valacchi *et al.*, 2009) and exposed to CAPs (25 or 100 μg/ml) for 3 or 12 h, in presence or absence of the iron chelator deferoxamine (DFO) (400 μM).

Cytotoxicity Determination

After CAPs exposure, culture media was collected at different time points (24 and 48 h). Cytotoxicity was determined by lactate dehydrogenase (LDH) release in the media, measured by enzymatic assay: in the first step NAD^+ is reduced to $NADH/H^+$ by the LDH-catalyzed conversion of lactate to pyruvate; in the second step the catalyst (diaphorase) transfers H/H^+ from $NADH/H^+$ to tetrazolium salt which is reduced to formazan. The amount of LDH in the supernatant was determined and calculated according to kit supplier's instructions (EuroClone, Milan, Italy). All tests were performed in triplicate. Results are express as percentage of change relative to control values.

PM Scanning Electron Microscopy (SEM)

The size, morphology, and composition of CAPs were analyzed by scanning electron microscopy (SEM). To characterize the PM used, the grid was coated with dry CAPs or a drop of CAPs suspension was air dried onto a carbon film coated SEM grid and assessed in a scan electron microscopy (Zeiss EVO 40). Three different gates were selected in each grid to performed energy-dispersive x-ray spectroscopy (EDS) at variable pressure (XVP SEM), accelerating voltage 20 kV. The INCA software was used for composition analysis (weight % and atomic %).

Hystochemistry

RHE tissue were fixed in 10% buffered formaldehyde and embedded in paraffin. For histological observation, the sections (4 μm thickness) were deparafinized in xylene and rehydrated in

alcohol gradients and then stained with hematoxylin and eosin (H&E).

Protein Extraction

At each time point, skin tissues were washed with ice-cold PBS and lysed in ice-cold lysis buffer (20 mM Tris pH 8, 150 mM NaCl, 1% Triton X-100, 1 mM sodium orthovanadate, 1 μg/ml leupeptin, 1 μg/ml aprotinin, 1 μg/ml pepstatin, 10 μg/ml PMSF, and 5 mM β-glycerophosphate) (Sigma, Milan, Italy). The suspensions were centrifuged at 10 000 × g for 15 min at 4°C, the pellet was discarded, and the supernatants were collected. Protein concentration was determined by the method of Bradford (Biorad, Milan, Italy).

4-Hydroxynonenal (4-HNE) Assay

Lipid peroxidation in RHE or HaCaT exposed to CAPs was evaluated by measuring 4-hydroxynonenal (4-HNE) levels using a commercially available kit (BioSource, Milan, Italy). Briefly, protein extracted from the RHE, were used as samples for the measurement of 4-HNE protein adduct, which was conducted as manufacturer's introduction. The measured amount of 4-HNE protein adduct was normalized with protein concentration measured with the Bradford method. A calibration curve was performed using 4-HNE standard. Results are expressed as μg 4-HNE/mg protein.

Measurement of Intracellular Reactive Oxygen Species (ROS) Levels

Intracellular ROS production was evaluated by oxidation of 2′-7′-dichloro-fluorescin diacetate (H2DCF-DA) to 2′-7′-dichloro-fluorescein (DCF). After CAPs treatment, HaCaT cells were washed with Kreb's Ringer Buffer (KRB) and incubated with 10 μM DCFH-DA (Sigma Aldrich) for 30 min at 37°C in the dark. Then, cells were washed with KRB and DCF fluorescence intensity was measured in the microplate reader at excitation wavelength of 485 nm and emission wavelength of 535 nm for 60 min. ROS production was expressed as arbitrary units of fluorescence (Arbitrary Units/min mg protein, where the actual protein content was evaluated in each well at the end of the assays. A blank, run in KBC with all reagents and without cells, was subtracted to all samples. In a set of experiments, after incubation with 10 μM DCFH-DA, cells were grown on coverslips and mounted on microscopy slides with antifade reagent and visualized by fluorescence microscopy.

Immunofluorescence

Paraffin embedded tissue sections (3 μm), which were cut transversally respect to RHE surface, were then deparaffinized and rehydrated. After antigen retrieval and blocking, as previously described (Valacchi *et al.*, 2011), the slides were incubated with the following antibodies: rabbit anti-IsoPro F2α (Abcam, Cambridge, UK), rabbit anti-cyclooxygenase 2 (COX2) (Cell Signaling Technology, Danvers, Massachusetts), rabbit anti-p65 subunit (SantaCruz Biotechnologies, Inc, Californias). Then, the slides were incubated with fluorochrome-conjugated secondary antibodies (goat anti-rabbit Alexa Fluor 488; Thermo Fisher Scientific Inc). The nuclei were counterstained by incubating the sections with 4′,6-diamidino-2-phenylindole (DAPI). Slides were mounted with Antifade. Negative controls were generated by omitting the primary antibody. Images were acquired and analyzed with a microscope Leica AF CTR6500HS (Microsystems) and analyzed with Image J software.

CYP1 Expression

Thirty microgram boiled proteins were loaded onto 10% sodium dodecyl sulphate-polyacrylamide electrophoresis gels and separated by molecular size. Gels were electro-blotted onto nitrocellulose membranes and then blots were blocked for 1 h in Tris-buffered saline, pH 7.5, containing 0.5% Tween20 and 3% milk. Membranes were incubated overnight at 4°C with the appropriate primary antibodies: CYP1A1 (Cell Signaling; Celbio, Milan, Italy), β-actin (Cell Signaling; Celbio). The membranes were then incubated with horseradish peroxidase-conjugated secondary antibody for 1 h, and the bound antibodies were detected by chemiluminescence (BioRad). β-Actin was used as loading control. Images of the bands were digitized and the densitometry analysis was performed using Image-J software. Results are expressed as relative to β-actin expression.

IL-1 Levels

IL-1α content was determined in the RHE culture media collected at different time points (24 or 48 h), using an ELISA kit (Thermo Scientific, Milan, Italy). It was done according to the manufacturer's instructions. The optical absorbance was measured with a microplate reader at 450 nm and correction at 530 nm. A calibration curve was performed using Recombinant Human IL-1α as standard. Results are expressed as pmol IL-1 α/ml.

TUNEL Assay

The terminal deoxynucleotidyl transferase-mediated deoxyuridine triphosphate nick end labeling (TUNEL) assay was used to detect apoptotic nuclei in the epidermis. The TUNEL staining assay kit (Apo-BrdU-IHC In Situ DNA Fragmentation Assay, BioVision, Inc, Milpitas, California) and all associated procedures were performed according to the manufacturer's instruction booklet. Briefly, skin tissues were fixed in 10% neutralized formalin and embedded in paraffin. Serial sections were deparaffinized, rehydrated, and incubated for 20 min at 37°C with proteinase K working solution (15 g/ml in 10 mM Tris-HCl, pH 7.5). After being rinsed twice with PBS, slices were incubated in hydrogen peroxide block for 10 min, and then 50 μl TUNEL reaction mixtures were added on the slices. Slices were incubated for 60 min at 37°C in a humidified atmosphere in the dark. After being rinsed with PBS, slices were added to 50 μl of converter-peroxidase and incubated in a humidified chamber for 30 min at 37°C, and then 50 μl of diaminobenzidine substrates was added and the slices were incubated for 10 min at 25°C. After being rinsed with PBS, slices were analyzed under a light microscope. Cells with shrunken brown-stained nuclei were considered positive.

Tissue Ultrastructural Analysis

RHE morphology was evaluated by transition electron microscopy (TEM). Tissues were fixed with 2.5% glutaraldehyde in 0.1 M sodium cacodylate buffer for 4 h at 4°C. They were then washed with 0.1 M cacodylate buffer (pH 7.4) 3 times and post-fixed in 1% osmium tetroxide and 0.1 M cacodylate buffer at pH 7.4 for 1 h at room temperature. The specimens were dehydrated in graded concentrations of ethanol and embedded in epoxide resin (Agar Scientific, 66 A Cambridge Road, Stanstead Essex, CM24 8DA, UK). RHE were then transferred to latex modules filled with resin and subsequently thermally cured at 60°C for 48 h. Semithin sections (0.5–1 μm thickness) were cut using an ultramicrotome (Reichard Ultracut S, Austria) stained with toluidine blue, and blocks were selected for thinning. Ultrathin sections of approximately 40–60 nm were cut and mounted onto

formvar-coated copper grids. These were then double-stained with 1% uranyl acetate and 0.1% lead citrate for 30 min each and examined under a transmission electron microscope, (Hitachi, H-800), at an accelerating voltage of 100 KV.

Statistical Analysis

Results were expressed as mean value ± SEM and represent the mean of triplicate determinations obtained in 4 separate experiments. ANOVA followed by Student-Newman-Keuls test was used to analyze differences among multiple experimental groups. Statistical significance was considered at $P < .05$.

RESULTS

Cytotoxicity Determination

As a first approach to evaluate the adverse effects of PM on skin tissues, LDH released measurements were carried out on RHE maintained media collected after different time points and CAPs doses exposure. As it is shown in Figure 1A, tissues exposed to 25 μg CAPs/ml presented increased LDH released only after 48 h (47%; $P < .05$), while RHE exposed to 100 μg CAPs/ml showed a significantly increased LDH release already at 24 h ($P < .01$) and continue up to 48 h ($P < .001$) after particles exposure when compared with control tissues (48 and 67% increased, respectively).

CAPs Characterization

Because CAPs exposure was able to induce skin tissues toxicity (Figure 1A); we perform CAPs characterization in regards to their morphology and composition by SEM. Elements present in CAPs samples are in accordance with previous description (Gurgueira *et al.*, 2002). As it is shown in Table 1, transition metals, mainly Fe, were observed through EDS analysis, and SEM images of CAPs showed particles size in a range between 2 and 6 μm (Figure 1B). However, it is worth it mentioning that the SEM images were carried out with dried particles, (making them susceptible to form agglomerates); while RHE exposure was performed using a CAPs suspension they can be categorized as $PM_{2.5}$ (aerodynamic diameter ≤ 2.5 μm).

Hystochemistry

As it is depicted in Figure 1C, in all samples, the basal, spinous, granulous and cornifyed epidermal layers were present. The treated epidermis did not show morphological alterations. In fact, there were no relevant differences among the groups (controls, 24 and 48 h-treated epidermis), the mitotic index (number of mitoses among 100 basal keratinocytes) did not significantly differ among the different groups.

Oxidative Damage Markers

One of the mechanisms suggested by which PMs exert adverse health effects is the oxidative stress occurrence, which may lead to lipid peroxidation. The F_2-α isoprostanes and 4-HNE levels are 2 of the most reliable oxidative damage markers. Isoprostanes are the product of arachidonic acid oxidation initiated by free radicals. As it is shown in Figure 2A, F_2-α isoprostanes levels, assessed by IsoPro F_2-α immunofluorescence integrate density, were clearly increased compared with the control group (control: 102 ± 1 IF), in the group exposed to 25 μg CAPs/ml for 48 h (52%) and RHE exposed to 100 μg CAPs/ml presented increased levels not only after 24 h (48%) exposure but after 48 h (89%) as well ($P < .001$). In addition, both CAPs doses RHE exposed for 48 h resulted significantly increase when compared with their dose matching groups exposed for 24 h ($P < .001$).

Regarding 4-HNE evaluation, another widely used phospholipid oxidative damage marker, only tissues exposed to 100 μg CAPs/ml for 24 and 48 h presented a 28% ($P < .001$) and 20% ($P < .01$), respectively, increased phospholipid oxidation level in comparison with control values (control: 0.25 ± 0.01 μg 4-HNE/mg protein) (Figure 2B).

As a proof of concept that one of the mechanisms involved in CAPs induced cell oxidative damage is via Fenton-like reaction initiated by transition metals present in CAPs surface, we have performed experiments using human keratinocytes, because cells are a better model to follow ROS formation. Keratinocytes were treated with 25 or 100 μg CAPs/ml for 3 or 12 h in presence or absence of 400 μM of the iron chelator . The data in Figure 2C clearly shows that CAPs induced an increased DCF signal at both 3 and 12 h (only the higher dose at late time point) and this was prevented by DFO treatment. In addition, the role of DFO in CAPs induced ROS formation was confirmed by immunofluorescence analysis as depict in Figure 2D. The presence of DFO was also able to decrease the 4-HNE formation in keratinocytes exposed to both CAPs doses for 12 h (Figure 2E). Altogether, these results confirm the hypothesis that transition metals present in CAPs can lead to the formation of ROS and lipid oxidation.

NFkB Activation

NFkB is a redox sensitive transcription factor that once activated, traslocates to the nucleus where can trigger the gene expression of inflammatory mediators. To evaluate if CAPs were able to activate this pathway, subunit p-65 immunohistochemistry was performed in RHE exposed to PM, and positive-stained nuclei percentage was assessed as NFkB activation parameter. As it is shown in Figure 3A, while no NFkB activation was observed in control RHE, CAPs exposure groups presented p-65 positive nuclei (25 μg CAPs/ml for 24 h: 28%; 25 μg CAPs/ml for 48 h: 26%; 100 μg CAPs/ml for 24 h: 32%; 100 μg CAPs/ml for 48 h: 38%).

CYP1A1 Expression

To evaluate the effects of PM exposure on cytochrome P450 hemoproteins, CYP1A1 expression was assessed by Western blot. CYP1A1 protein is a cytochrome P450 enzyme superfamily member which is involved in xenobiotics metabolism. Skin tissues exposed to 25 μg CAPs/ml for 24 h presented a 73% increased expression ($P < .01$) compared with control values (control: 1.5 ± 0.3 CYP1A1/β-actin ratio). None of the other CAPs-exposed groups showed changes relative to control (Figure 3B).

Inflammation Markers

The IL-1 isoforms play a key role in the inflammatory respond trigger by air pollutants. Among them, IL-1α has been associated with pro-inflammatory mechanisms. IL-1α released by skin tissues after CAPs treatment was measured by a spectrophotometric assay, using RHE maintenance media as samples. Results are presented in Figure 3C. Every CAPs experimental group showed IL-1α levels significantly higher than the group exposed to the control saline. In addition RHE exposed to 100 μg CAPs/ml presented higher IL-1α levels after 24 h, while RHE treatment with 100 μg CAPs/ml showed higher values at 48 h in relation to 24 h exposed to the same dose ($P < .01$).

PM-adverse health effects could also initiate inflammatory and signaling pathways where COX-2 is involved. Moreover, the expression of this enzyme is regulated by inflammatory

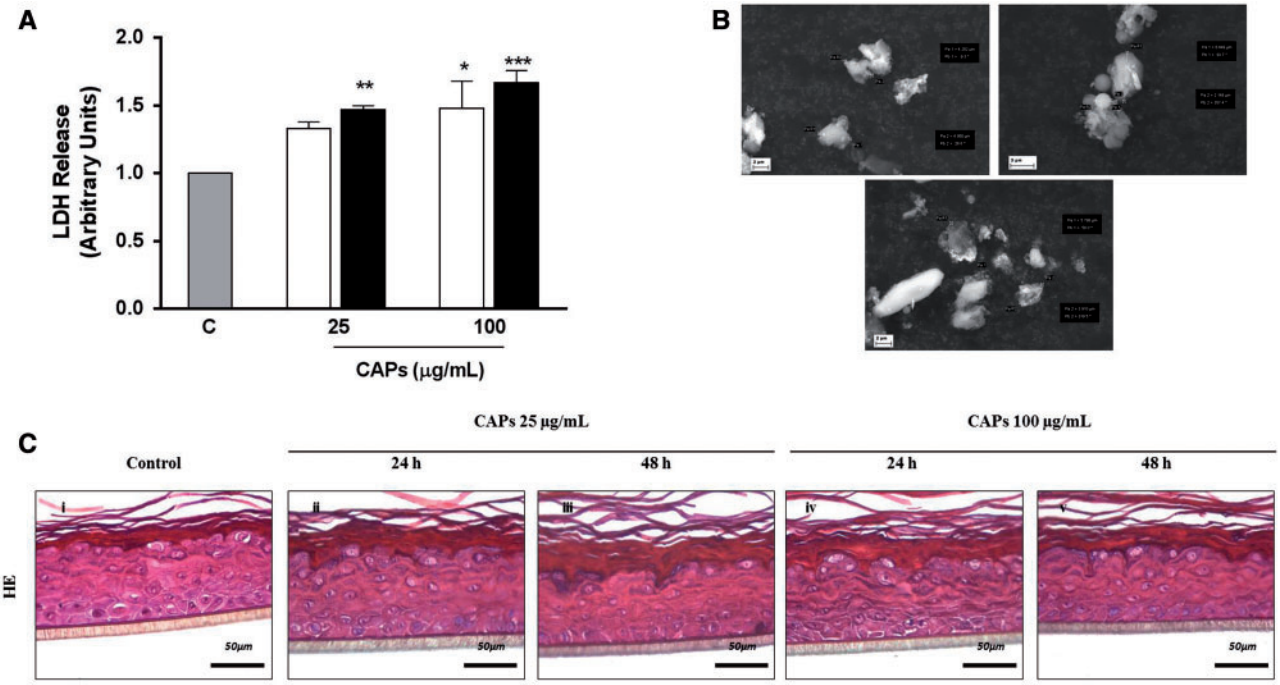

FIG. 1. Air pollution particles smaller than 2.5 μm increase skin tissue cytotoxicity. A, Cytotoxicity evaluation by lactate dehydrogenase release in reconstructed human epidermis (RHE) maintenance media after 24 (□) or 48 h (■) exposure to 25 or 100 μg CAPs/ml measured by an enzymatic assay. Data are presented as mean ± SEM, $n \geq 3$.* $P < .05$; ** $P < .01$; *** $P < .01$ versus control group. B, CAPs morphology analysis. Scanning electron microscopy (SEM) images. × 10000. C, Skin tissue morphology evaluation by hematoxilin-eosin staining.

TABLE 1. CAPs Composition Evaluated by EDS Analysis

Element	Weight %
C	44.89
O	38.40
Mg	0.15
Al	0.37
Si	14.75
P	0.20
S	0.55
K	0.11
Ca	0.34
Fe	0.23
Total	100.00

mediators such as IL-1α. Therefore, it seems relevant to assess COX-2 expression through immunofluorescence. As it can be seen in Figure 3D, compared with control values, immunofluorescences integrate density quantification results significantly higher in CAPs groups' regardless dose or time exposure. Forty-eight hour exposure to CAPs produce increased expression in comparison with 24 h group only after the lower dose exposure ($P < .001$).

DNA Alterations

PM-generated oxidative metabolism and inflammatory mediators may also modulate genes involved in the control of the cell cycle and apoptosis and direct DNA alterations. As it can be observed in Figure 4 through TUNEL assay, no signal could be detected in control RHE, while every CAPs-exposed tissue showed TUNEL positive nuclei, indicating double- and single-stranded DNA fragmentation resulting from apoptotic signaling cascades.

Tissue Ultrastructural Analysis

With the aim of clarifying the interactions between CAPs and skin tissue ultrastructural analysis by TEM was performed. Interestingly, we observed particles inside the tissue after 100 μg CAPs/ml. Slices from 24 h exposed RHE presented CAPs in the upper cell, near corneous layer, whereas 48 h after PM treatment particles were also found in deeper cell layers (Figure 5).

DISCUSSION

Several researchers have established a direct correlation between increased environmental air PM levels and adverse health effects (Dominici *et al.*, 2006). People may be exposed to different air pollutants via inhalation, ingestion, and dermal contact. Nowadays, epidemiological and clinical studies are progressively more interested in skin outcomes after PM exposure (Ahn, 2014). However, scarce data is available regarding the mechanisms exert by air pollution on cutaneous tissues. In this scenario, the aim of this study was to clarify the phenomena underlying the toxic pathways initiated by CAPs exposure in cutaneous tissues and to do so we have performed experiment in a tree dimensional skin culture model (RHE).

Our data show that CAPs exposure significantly affected RHE viability, as demonstrated by LDH release. Although, there was a dose-time relationship because when RHE were exposed to the lower dose of particles, skin tissues required more time to develop cytotoxicity. It is accepted that exposure to air pollution PM triggers an inflammatory response, endothelial activation, and oxidative stress (Chen and Lipmann, 2009). Injury to diverse

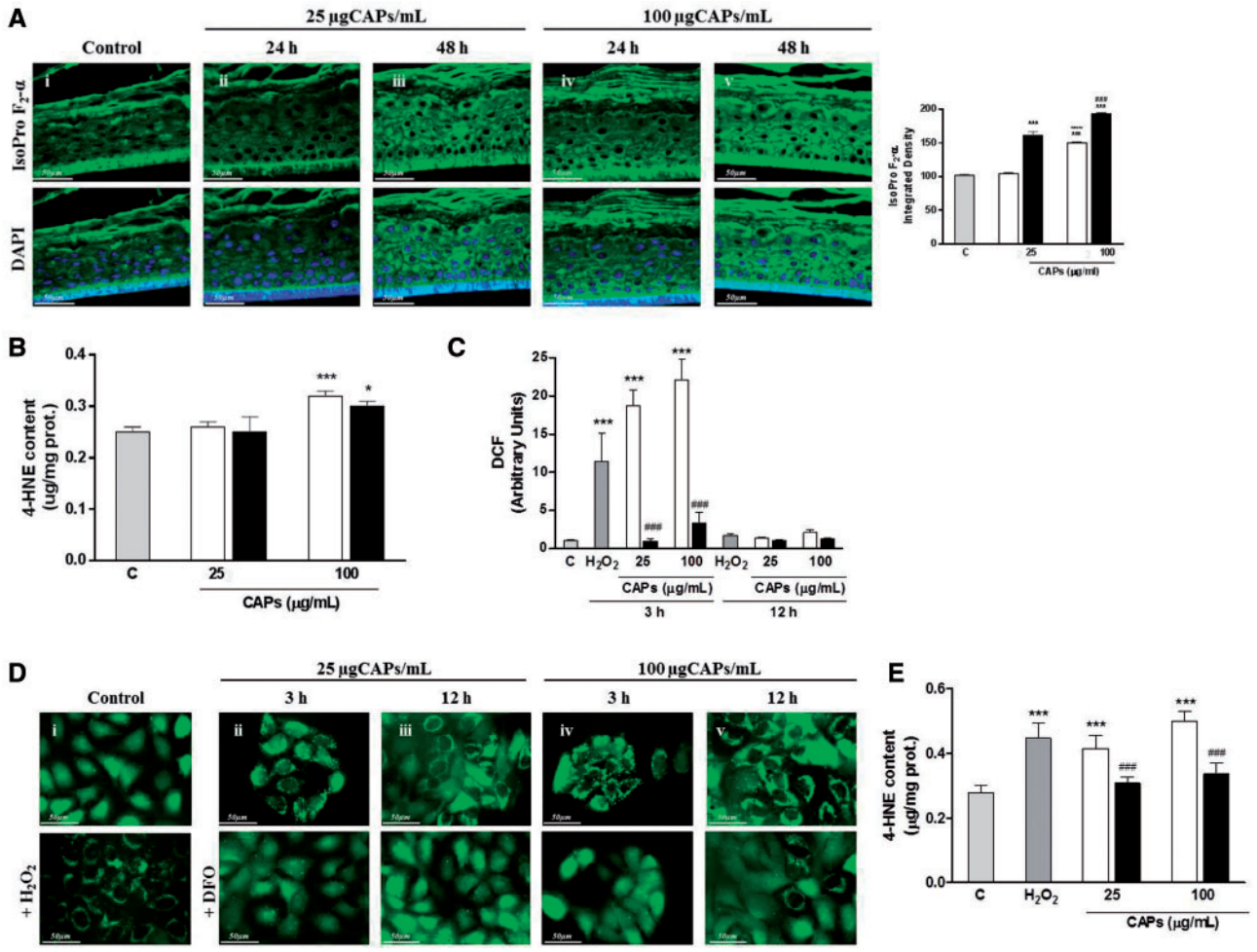

FIG. 2. CAPs exposure increase oxidative damage occurrence through increased reactive oxygen species (ROS) production. A, Macromolecules oxidation measured by isoprostanes expression in RHE slices (top panels) and their correspondent DAPI signal (lower panels) in i) control slices; ii) after 24 h exposure to 25 µg CAPs/ml; iii) after 48 h exposure to 25 µg CAPs/ml; iv) after 24 h exposure to 100 µg CAPs/ml; and v) after 24 h exposure to 100 µg CAPs/ml. Integrated density quantification. *** $P < .001$ versus control group; ### $P < .001$ versus 24 h exposure to 25 µg CAPs/ml; ~~~ $P < .001$ versus 24 h exposure to 100 µg CAPs/ml group. B, Oxidative damage assessed through 4-hydroxynonenal (4-HNE) content in RHE after 24 (□) or 48 h (■) exposure to 25 or 100 µg CAPs/ml measured by an enzymatic assay. Data is presented as mean ± SEM, $n \geq 3$.* $P < .05$; *** $P < .01$ versus control group. C, ROS production evaluated by 2′-7′-dichloro-fluorescein (DCF) oxidation in HaCaT cell exposed to 25 or 100 µg CAPs/ml for 3 or 12 h, in absence (□) or presence (■) of 400 µM of deferoxamine (DFO). H_2O_2 was used as a positive control. Data is presented as mean ± SEM, $n \geq 3$. *** $P < .01$ versus control group; ### $P < .01$ versus respective group without DFO. D, Intracellular ROS levels visualized by DCF fluorescent microscopy in HaCat cell exposed to 25 or 100 µg CAPs/ml for 3 or 12 h, in absence or presence of 400 µM of DFO. H_2O_2 was used as a positive control. E, Oxidative damage assessed through 4-HNE content in HaCat cells measured by an enzymatic assay after 10 h exposure to 25 or 100 µg CAPs/ml in absence (□) or presence (■) of 400 µM of DFO. H_2O_2 was used as a positive control. Data are presented as mean ± SEM, $n \geq 3$. *** $P < .01$ versus control group; ### $P < .01$ versus respective group without DFO.

organs after air pollution contact has been suggested to be generated not only from the particles themselves but also mainly from the chemicals coated on their surface. Therefore, particles physical properties characterization becomes relevant. Concerning PM size, we found that CAPs are included in the fine groups considering the aerodynamic diameter observed (< 2.5 µm). Thanks to their small size but large surface per unit mass, they become highly reactive in biological surfaces and structures (Donaldson *et al.*, 2005). The smaller the particles are the higher is the diameter/surface area rate where molecules could be absorbed. Therefore, fine and ultrafine particles fraction seem to be of major concern from the health perspective (Delfino *et al.*, 2005). PM can act as carrier of both organic and inorganic compounds found in the particle's core. In agreement with previous CAPs characterization (Ghelfi *et al.*, 2010; Gurgueira *et al.*, 2002) we also observed the presence of transition metals, such as Fe, in the surface of the PM. Due to their ability to participate in Fenton-like reaction, Fe could contribute to an increase ROS production, which in turn, might be able to initiate molecular mechanisms leading to oxidative damage within the tissue as we have demonstrated by the use of iron chelator in human keratinocytes. Besides transition metals, other compounds present in air pollution, such as semiquinones, lipopolysaccaride, hydrocarbon, and ultrafine constituents, may also exert oxidative stress by presenting or by stimulating the cells to produce ROS. The augmented oxidant species production may overwhelm the enzymatic and nonenzymatic antioxidant defenses capacity, thus leading to deleterious effects (Bickers and Athar, 2006). Phospholipids are the macromolecule more sensitive to changes in the redox cellular status after PM exposure (Magnani *et al.*, 2001). CAPs exposure showed increased levels of arachidonic acid oxidation, as seen by IsoPro F_2-α immunofluorescence. The

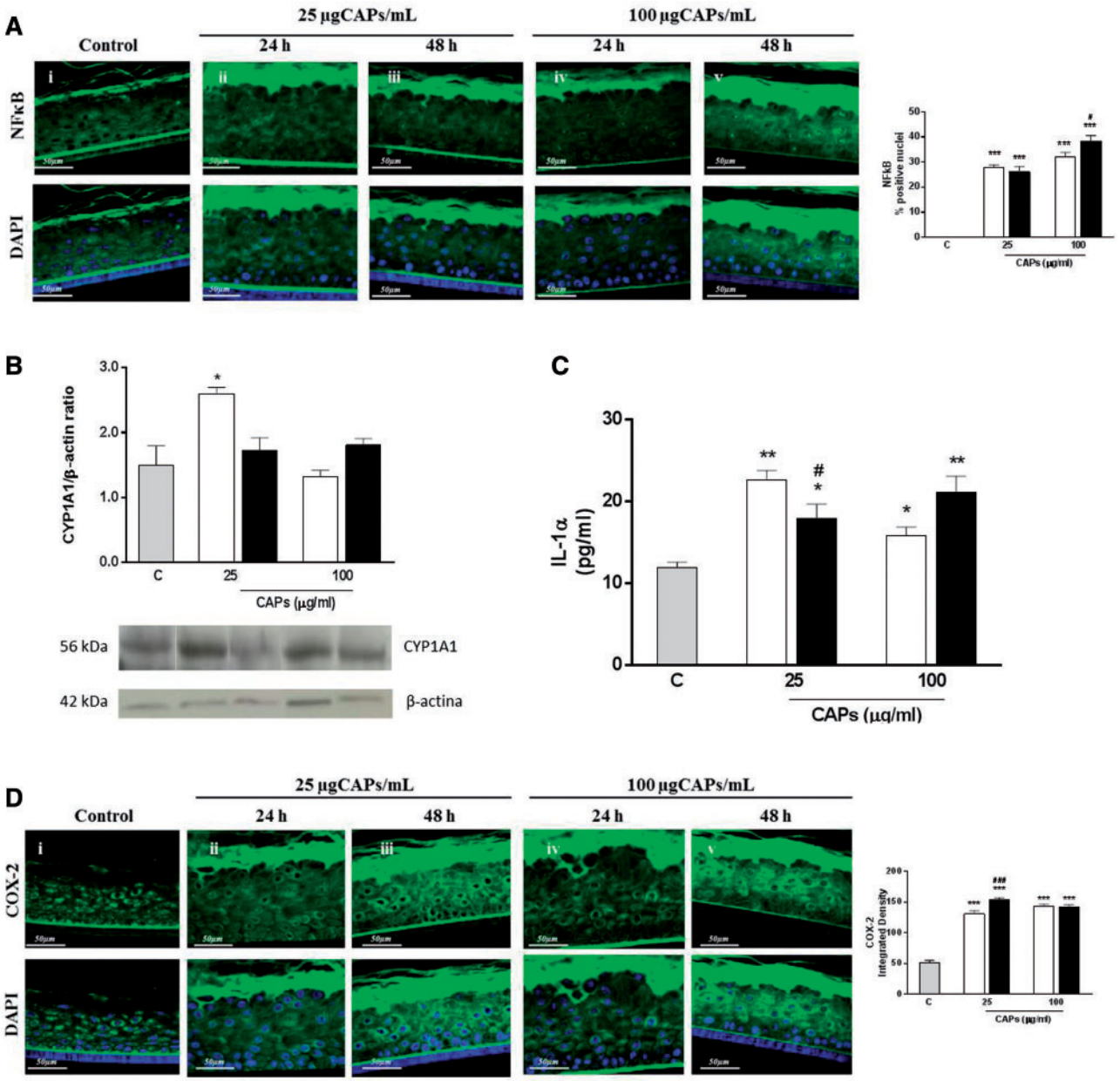

FIG. 3. CAPs exposure induces pro-inflammatory responses. A, NFκB traslocation to nucleus in RHE slices (top panels) and their correspondent DAPI signal (lower panels) in i) control slices; ii) after 24 h exposure to 25 µg CAPs/ml; iii) after 48 h exposure to 25 µg CAPs/ml; iv) after 24 h exposure to 100 µg CAPs/ml; and v) after 24 h exposure to 100 µg CAPs/ml. Integrated density quantification. *** $P < .001$ versus control group; # $P < .05$ versus 24 h exposure to 25 µg CAPs/ml. B, CYP1A1 expression in RHE protein extraction after 24 (□) or 48 h (■) exposure to 25 or 100 µg CAPs/ml measured by Western blot. Data are presented as mean ± SEM, $n \geq 3$.* $P < .05$ versus control group. C, Interleukin -1 release in RHE maintenance media after 24 (□) or 48 h (■) exposure to 25 or 100 µg CAPs/ml measured by an enzymatic assay. Data are presented as mean ± SEM, $n \geq 3$.* $P < .05$; ** $P < .01$ versus control group. D, cyclooxygenase-2 expression in RHE slices (top panels) and their correspondent DAPI signal (lower panels) in i) control slices; ii) after 24 h exposure to 25 µg CAPs/ml; iii) after 48 h exposure to 25 µg CAPs/ml; iv) after 24 h exposure to 100 µg CAPs/ml; and v) after 24 h exposure to 100 µg CAPs/ml.

arachidonic acid once is oxidized forms other radical compounds, which are able to increase the phospholipid oxidation and lead to further omega-6 PUFA oxidation as demonstrated by the increased levels of 4-HNE.

In addition to the earlier observations, it is accepted that oxidative stress is also involved in triggering pro-inflammatory pathways by activating redox sensitive transcription factor, such as NFkB, that can contribute to the deleterious effects of PM in multicellular organisms (Marchini *et al.*, 2014). Once activated, NFkB can translocate to nucleus, as it is observed after CAPs exposure, and transcribes for several pro-inflammatory genes such as IL-1α and COX-1. Consistently, we have observed increase levels of the pro-inflammatory markers COX-2 and IL-1α in skin tissues exposed to PM.

Increased ROS production might imitate the nuclear factor (erythroid-derived 2)-like 2 (Nrf2) pathway, and a possible cross talk between Nrf2 and NFkB activation has been also suggested. Although the exact sequence of events that might activate these 2 pathways is still not clear. Indeed, if from 1 side PM exposure is associated with increased oxidative stress and therefore a

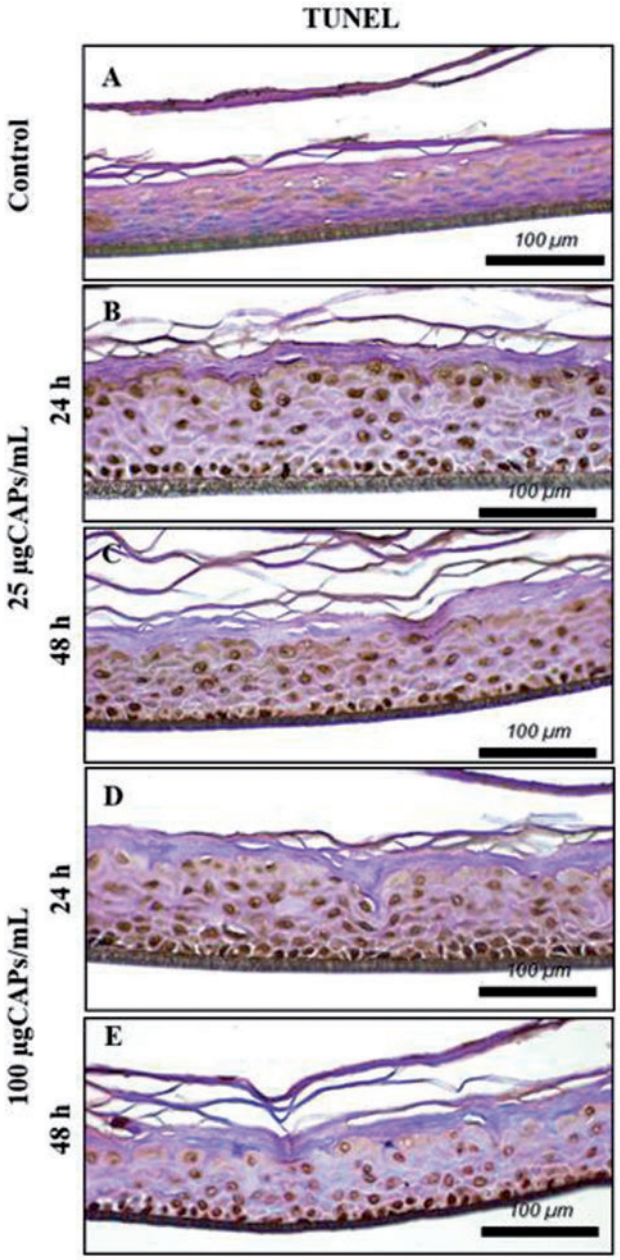

FIG. 4. Oxidative and inflammatory mechanisms initiated after CAPs exposure lead to apoptotic cells in skin tissue. Apoptotic nuclei detection in RHE slices, evaluated by terminal deoxynucleotidyl transferase-mediated deoxyuridine triphosphate nick end labelling assay in (A) control slices; (B) after 24 h exposure to 25 µg CAPs/ml; (C) after 48 h exposure to 25 µg CAPs/ml; (D) after 24 h exposure to 100 µg CAPs/ml; and (E) after 24 h exposure to 100 µg CAPs/ml.

possible Nrf2 activation and induction of the "antioxidant defense system" that could decrease ROS levels leading to decreased NFkB activation; from another side, exposure to air pollutants is also associated with an increased inflammatory response NFkB mediated (Anderson *et al.*, 2012; Tsai *et al.*, 2012). In addition, it is well documented that knocking out or silencing Nrf2 increases NFkB activation. This is due, in part, to a decrease in antioxidant defensive enzymes transcription, including HO-1, NQO1, thioredoxin, and GSH (Thimmulappa *et al.*, 2006; Wakabayashi *et al.* 2010). Furthermore, Nrf2 can also antagonize NFkB binding to its cis element (Wakabayashi *et al.* 2010). Indeed, there is much cross talk between Nrf2 and NFkB pathways, including inhibition of Nrf2 by NFkB, which can decrease availability of Nrf2 coactivators needed for transcription (Matthews *et al.*, 1992). Therefore, it is possible that PM, via their ability to induced oxidative stress, are able to activate both systems (Nrf2 and NFkB) independently and then only the balance between the "antioxidants defense system" transcribed genes by Nrf2 and the "inflammatory genes" transcribed by NFkB, will result in a more or less pronounced pro-inflammatory responses.

Different hypothesis has been proposed concerning the initiation of the PM detrimental effects on cutaneous tissues. This could be due to an indirect effect by an outside-inside signaling cascade. As it has been mentioned, PM, especially smaller particles, may carry metal ions and/or organic compounds such as PAHs which are highly lipophilic and, both can penetrate the skin surface (Vierkötter *et al.*, 2010). Although it has been suggested that different air pollutant may have specific effects, it is worthily to observe that other pollutant like O_3, which exert indirect toxic mechanism on skin (Fortino *et al.*, 2007; Valacchi *et al.*, 2002), and recently has been showed that O_3 increased activation of the detoxifying enzyme cytochrome p450 via AhR receptor (Afaq *et al.*, 2009). This is in agreement with our observations in RHE PM-exposed tissues. Moreover PAHs are potent ligands for the AhR receptor, expressed by both keratinocytes and melanocytes, which upregulates pro-inflammatory mediators an increase ROS production (Fritsche *et al.*, 2007; Jux *et al.*, 2011).

On the other hand, PM-adverse health effects initiation involve penetration of PM into the skin. Nowadays, it is accepted that increased levels of ambient PM could enter skin either through hair follicles or transepidermally (Lademann *et al.*, 2005). The ability of particles to enter skin tissue was also evaluated in previous studies. Although Tinkle *et al.* (2003) have showed that only particles smaller than 0.1 µm were able to penetrate the stratum corneum of human skin, we believed that the particles used in this study were substantially different from the ones that we have used in the present work. Taking into account the physicochemical characteristics of CAPs it is clear that they are highly reactive toward biological surfaces. Their ability to disturb the skin barrier function relies on the amount of particles in contact with the corneocytes and on the exposure time period. According to the ultrastructural analysis only higher doses of CAPs can break through the stratum corneum and be found in deeper cell layers 48 h after exposure. It is worth it to mention that our results were performed in a 3 dimensional skin model and not in an *in vivo* model.

However, it is interesting that regardless the initiation mechanisms, the present PM exposure model, triggers apoptosis occurrence in every group treated, which means that CAPs leads to skin damage associated with the development of various skin diseases (Valacchi *et al.*, 2012).

In this study, we provide evidence that PM develop cutaneous damage not only directly, once particles reach deeper layers in the epidermis, but also indirectly, triggering a signaling pathway. Oxidative stress and an inflammatory response seem to be important steps in the CAPs-toxic mechanisms.

In conclusion, the present work provides new insights on the possible mechanisms that are involved in PM induced skin damage, suggesting a cascade of effects that are driven by inflammatory processes and oxidative damage.

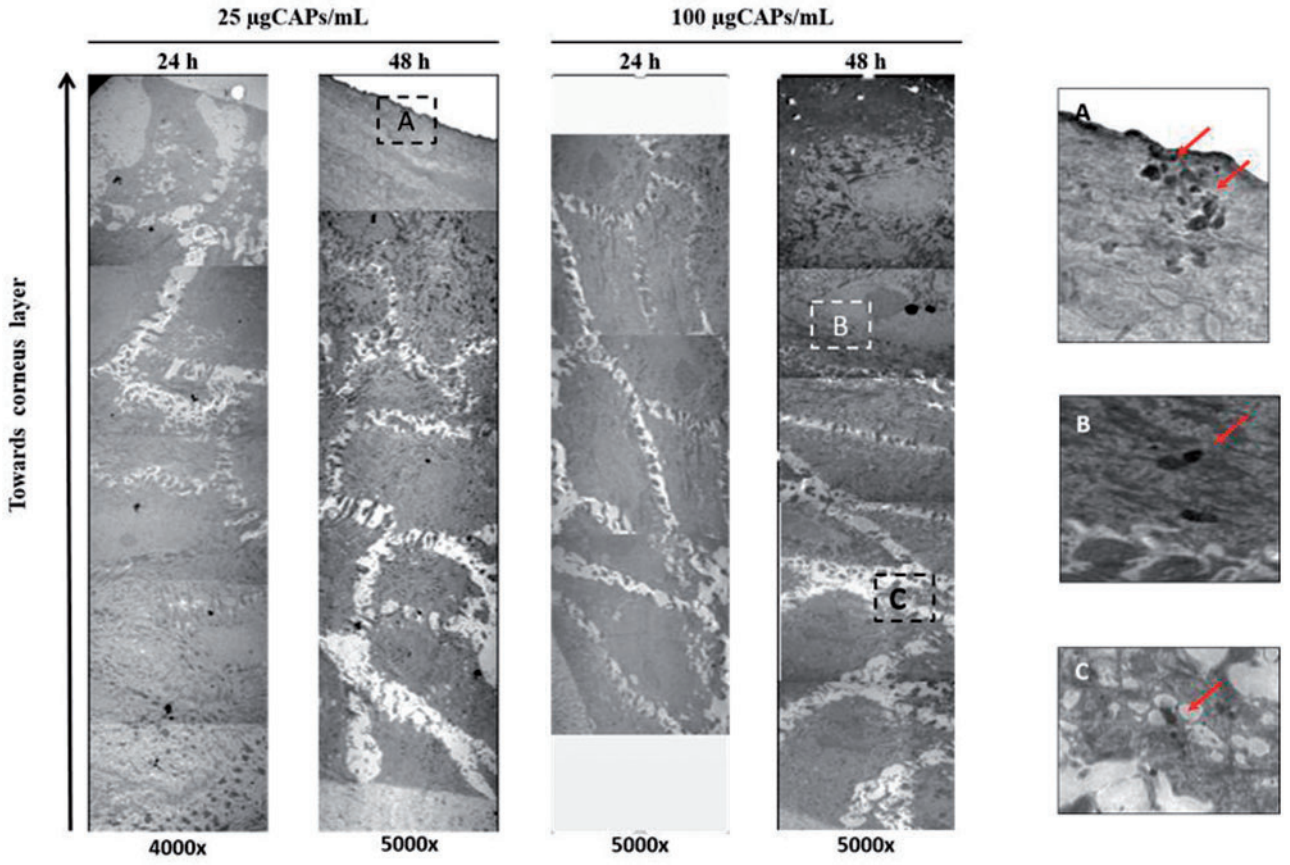

FIG. 5. CAPs are able to penetrate skin tissue. Ultrastructural analysis by transition electron microscopy (TEM) in RHE slices after 24 h exposure to 25 µg CAPs/ml; after 48 h exposure to 25 µg CAPs/ml; after 24 h exposure to 100 µg CAPs/ml; or after 24 h exposure to 100 µg CAPs/ml. A–C boxes correspond to magnification of their respective selected zones showed in the images, arrows point the zone were CAPs can be observed.

ACKNOWLEDGMENT

The authors are thankful to Mr. Andrea Margutti for technical assistance.

REFERENCES

Afaq, F., Zaid, M. A., Pelle, E., Khan, N., Syed, D. N., Matsui, M. S., Maes, D., and Mukhtar, H. (2009). Aryl hydrocarbon receptor is an ozone sensor in human skin. *J. Invest. Dermatol.* **129**, 2396–2403.

Ahn, K. (2014). The role of air pollutants in atopic dermatitis. *J. Allergy Clin. Immunol.* **134**, 993–999.

Anderson, J. O., Thundiyil, J. G., and Stolbach, A. (2012). Clearing the air: A review of the effects of particulate matter air pollution on human health.*J. Med. Toxicol.* **8**, 166–175.

Baroni, A., Buommino, E., De Gregorio, V., Ruocco, E., Ruocco, V., and Wolf, R. (2012). Structure and function of the epidermis related to barrier properties. *Clin. Dermatol.* **30**, 257–262.

Bickers, D. R., and Athar, M. (2006). Oxidative stress in the pathogenesis of skin disease. *J. Invest. Dermatol.* **126**, 2565–2575.

Brunekreef, B., and Holgate S. T. (2002). Air pollution and health. *Lancet* **360**, 1233–1242.

Chen, L. C., and Lipmann, M. (2009). Effects of metals within ambient air particulate matter (PM) on human health. *Inhal. Toxicol.* **21**, 1–31.

Delfino, R. J., Sioutas, C., and Malik, S. (2005). Potential role of ultrafine particles in associations between airborne particle mass and cardiovascular health. *Environ. Health Perspect.* **113**, 934–946.

Dominici, F., Peng, R. D., Bell, M. L., Pham, L., McDermott, A., Zeger, S. L., and Samet, J. M. (2006). Fine particulate air pollution and hospital admission for cardiovascular and respiratory diseases. *JAMA* **295**, 1127–1134.

Donaldson, K., Tran, L., Jimenez, L. A. Duffin, R., Newby, D. E., Mills, N., MacNee, W., and Stone, V. (2005). Combustion-derived nanoparticles: A review of their toxicology following inhalation exposure. *Part. Fibre Toxicol.* **2,** 10.

Fortino, V., Maioli, E., Torricelli, C., Davis, P., and Valacchi, G. (2007). Cutaneous MMPs are differently modulated by environmental stressors in old and young mice. *Toxicol. Lett.* **173**, 73–9.

Fritsche, E., Schäfer, C., Calles, C., Bernsmann, T., Bernshausen, T., Wurm, M., Hübenthal, U., Cline, J. E., Hajimiragha, H., Schroeder, P., *et al.* (2007). Lightening up the UV response by identification of the arylhydrocarbon receptor as a cytoplasmatic target for ultraviolet B radiation. *Proc. Natl. Acad. Sci. U.S.A.* **104**, 8851–8856.

Fujishima, H., Satake, Y., Okada, N., Kawashima, S., Matsumoto, K., and Saito, H. (2013). Effects of diesel exhaust particles on primary cultured healthy human conjunctival epithelium. *Ann. Allergy Asthma Immunol.* **110**, 39–43.

Ghelfi, E., Wellenius, G. A., Lawrence, J., Millet, E., and Gonzalez-Flecha, B. (2010). Cardiac oxidative stress and dysfunction by fine concentrated ambient particles (CAPs) are mediated by angiotensin-II. *Inhal. Toxicol.* **22**, 963–972.

Ghio, A. J., and Huang Y. C. (2004). Exposure to concentrated ambient particles (CAPs): A review. *Inhal. Toxicol.***16**, 53–59.

Goldsmith, C. A., Imrich, A., Danaee, H., Ning, Y. Y., and Kobzik, L. (1998). Analysis of air pollution particulate-mediated oxidant stress in alveolar macrophages. *J. Toxicol. Environ. Health A* **54**, 529–545.

Gurgueira, S. A., Lawrence, J., Coull, B., Krisha Murthy, G. G., González-Flecha, B. (2002). Rapid increases in the steady-state concentration of reactive oxygen species in the lungs and heart after particulate air pollution inhalation. *Environ. Health Perspect.* **110**, 749–755.

Jux, B., Kadow, S., Luecke, S., Rannug, A., Krutmann, J., and Esser, C. (2011). The aryl hydrocarbon receptor mediates UVB radiation-induced skin tanning. *J. Invest. Dermatol.* **131**, 203–210.

Kim, J., Kim, E. H., Oh, I., Jung, K., Han, Y., Cheong, H. K., and Ahn, K. (2013). Symptoms of atopic dermatitis are influenced by outdoor pollution. *J. Allergy Clin. Immunol.* **132**, 495–497.

Lademann, J., Otberg, N., Jacobi, U., Hoffman, R. M., and Blume-Peytavi, U. (2005). Follicular penetration and targeting. *J. Investig. Dermatol. Symp. Proc.* **10**,301–3.

Li, N., Xia, T., and Nel, A. E. (2008). The role of oxidative stress in ambient particulate matter induced lung diseases and its implications in the toxicity of engineered nanoparticles. *Free Radic. Biol. Med.* **44**, 1689–1699.

Magnani, N. D., Marchini, T., Tasat, D. R., Alvarez, S., and Evelson, P. A. (2001). Lung oxidative metabolism after exposure to ambient particles. *Biochem. Biophys. Res. Commun.* **412**, 667–72.

Magnani, N. D., Marchini, T., Vanasco, V., Tasat, D. R., Alvarez, S., and Evelson, P. (2013). Reactive oxygen species produced by NADPH oxidase and mitochondrial dysfunction in lung after an acute exposure to residual oil fly ashes. *Toxicol. Appl. Pharmacol.* **270**, 31–38.

Marchini, T., Magnani, N. D., Paz, M. L., Vanasco, V., Tasat, D., González Maglio, D. H., Alvarez, S., and Evelson, P. A., (2014). Time course of systemic oxidative stress and inflammatory response induced by an acute exposure to Residual Oil Fly Ash. *Toxicol. Appl. Pharmacol.* **274**, 274–282.

Mastrofrancesco, A., Alfè, M., Rosato, E., Gargiulo, V., Beatrice, C., Di Blasio, G., Zhang, B., Su, D. S., Picardo, M., and Fiorito, S. (2014). Proinflammatory effects of diesel exhaust nanoparticles on scleroderma skin cells. *J. Immunol. Res.* **2014**, 138751.

Matthews, J. R., Wakasugi, N., Virelizier, J. L., Yodoi, J., and Hay, R. T. (1992). Thioredoxin regulates the DNA binding activity of NFkB by reduction of a disulphide bond involving cysteine 62. *Nucleic Acids Res.* **20**, 3821–3830.

Nel, A. (2005). Atmosphere. Air pollution-related illness: Effects of particles. *Science* **308**, 804–806.

Nel, A., Xia, T., Mädler, L., and Li, N. (2006). Toxic Potential of Materials at the Nanolevel. *Science* **311,** 622–627.

Pierdominici, M., Maselli, A., Cecchetti, S., Tinari, A., Mastrofrancesco, A., Alfè, M., Gargiulo, V., Beatrice, C., Di Blasio, G., Carpinelli, G., *et al.* (2014). Diesel exhaust particle exposure in vitro impacts T lymphocyte phenotype and function. *Part. Fibre Toxicol.* **14**, 11–74.

Pillai, S., Oresajo, C., and Hayward, J. (2005). Ultraviolet radiation and skin aging: Roles of reactive oxygen species, inflammation and protease activation, and strategies for prevention of inflammation-induced matrix degradation—A review. *Int. J. Cosmet. Sci.* **27**, 17–34.

Rhoden, C. R., Rhoden, C. R., Lawrence, J., Godleski, J. J., and González-Flecha, B. (2004). N-acetylcysteine prevents lung inflammation after short-term inhalation exposure to concentrated ambient particles. *Toxicol. Sci.* **79**, 296–303.

Schröder, P., Schieke, S. M., and Morita, A. (2006). Premature skin aging by infrared radiation, tobacco smoke and ozone. In *Skin Aging* (B. A. Gilchrest and J. Krutmann, Eds.), pp 45–55. Springer-Verlag Editorial, New York, NY.

Sioutas, C., Koutrakis, P., and Burton, R. M. (1995). A technique to expose animals to concentrated fine ambient aerosols. *Envrion. Health Perpect.* **103**, 172–177.

Soeur, J., Eilstein, J., Léreaux, G., Jones, C., and Marrot, L. (2015). Skin resistance to oxidative stress induced by resveratrol: From Nrf2 activation to GSH biosynthesis. *Free Radic. Biol. Med.* **78**, 213–23.

Thimmulappa, R. K., Lee, H., Rangasamy, T., Reddy, S. P., Yamamoto, M., Kensler, T. W., and Biswal, S. (2006). Nrf2 is a critical regulator of the innate immune response and survival during experimental sepsis. *J. Clin. Invest.* **116**, 984–995.

Tinkle, S., Antonini, J. A., Rich, B. A., Roberts, J. R., Salmen, R., DePree, K., and Adkins, E. J. (2003). Skin as a route of exposure and sensitization in chronic beryllium disease. *Environ. Health Perspect.* **111**, 1202–1208.

Tsai, D. H., Amyai, N., Marques-Vidal, P., Wang, J. L., Riediker, M., Mooser, V., Paccaud, F., Waeber, G., Vollenweider, P., and Bochud, M. (2012). Effects of particulate matter on inflammatory markers in the general adult population. *Part. Fibre Toxicol.* **9**, 24.

Valacchi, G., Lim, Y., Belmonte, G., Miracco, C., Zanardi, I., Bocci, V., Travagli, V. (2011). Ozonated sesame oil enhances cutaneous wound healing in SKH1 mice. *Wound Repair Regen.* **19**, 107–115.

Valacchi, G., Pecorelli, A., Mencarelli, M., Carbotti, P., Fortino, V., Muscettola, M., and Maioli, E. (2009). Rottlerin: A multifaced regulator of keratinocyte cell cycle. *Exp. Dermatol.* **18**, 516–521.

Valacchi, G., Sticozzi, C., Pecorelli, A., Cervellati, F., Cervellati, C., and Maioli, E. (2012). Cutaneous responses to environmental stressors. *Ann. NY Acad. Sci.* **1271**, 75–81.

Valacchi, G., van der Vliet, A., Schock, B. C., Okamoto, T., Obermuller-Jevic, U., Cross, C. E., and Packer, P. (2002). Ozone exposure activates oxidative stress responses in murine skin. *Toxicology* **179**, 163–170.

Vierkötter, A., Schikowski, T., Ranft, U., Sugiri, D., Matsui, M., Kramer, U., and Krutmann, J. (2010). Airborne particle exposure and extrinsic skin aging. *J. Invest. Dermatol.* **130**, 2719–2726.

Wakabayashi, N., Slocum, S. L., Skoko, J. J., Shin, S., and Kensler, T. W. (2010). When NRF2 talks, who's listening? *Antioxid. Redox Signal.* **13**, 1649–1663.

World Health Organization (WHO). 2014. Burden of disease from the joint effects of household and ambient air pollution for 2012. Public Health, Social and Environmental Determinants of Health Department, WHO.